J Electr Eng Technol.2018; 13(4): 1578-1585
http://doi.org/10.5370/JEET.2018.13.4.1578

ISSN(Print) 1975-0102
ISSN(Online) 2093-7423

Low Cost Motor Drive Technologies for ASEAN Electric Scooter

V. Tran Tuan†, S. Kreuawan*, P. Somsiri* and P. Nguyen Huy**

Abstract – This work investigates two different motor drive technologies, switched reluctance motor (SRM) and induction motor (IM). They are designed optimally to meet the desired performances for electric scooters. The comparison of both motors is described in terms of performances and material cost. With the similar constraint, induction motor performs slightly better than switched reluctance motor. But this must be traded-off with higher weight and cost. Both drive systems are, however, suitable for electric scooter application. Finally, the range simulations are conducted on a European urban driving cycle, ECE15 driving cycle and a more realistic cycle, Bangkok driving cycle. The e-scooter ranges are varied from 36 to 109 km depending on driving cycle, motor technology and number of passengers.

Keywords: Electric scooter (E-scooter), High Speed, Driving cycle, Switched Reluctance Motor, Asynchronous (Induction) Motor, Finite Element Analysis.

1. Introduction

In developing ASEAN countries, there is traffic congestion, not sufficient and low quality public transportation, income inequality problem. Therefore, scooters are one of main transportation modes in the major cities such as Bangkok and Hanoi. Pollution problem becomes more severe with tens of millions of scooters in the city. Electric scooter (e-scooter) might be a good solution. Despite their high price, the e-scooters, available in the market, provide low performances (limited by their top speed of 50 km/h). They are not suitable for everyday use as the internal combustion engine (ICE) scooter replacement. They need to be higher performances and lower price, in order to gain more customers.

This work focuses on electric traction motor, which is a key component of e-scooter. Good driving performances can be achieved by well-designed torque-speed motor characteristic. High efficiency motor increases driving range with the same battery capacity. Low motor cost makes more profit or lower end-user price. Both low cost machines, induction motor (IM) and switched reluctance motor (SRM), are well known by their simple manufacturing and reliability compared to the permanent magnet synchronous motor (PMSM) [1-7]. They will be good candidates for e-scooter application developed for the ASEAN emerging markets.

In the first section, the e-scooter specifications will be detailed. The following section will describe the design process of both machine technologies. In the third section, results on machine sizing, performances taking into account the optimal control parameters, range on driving cycles, and material cost of both motors will be then compared.

2. E-Scooter Specifications

2.1 E-scooter performance specifications

Electric drive system is designed with the target performance comparable to the conventional internal combustion engine (ICE) scooter size 110 - 120 cm^3 for everyday and general-purpose uses. For example, the e-scooter must be able to climb the inclination of 25 - 40 % depending of the number of passenger. Its maximum speed is 80 km/h for 1 driver and 70 km/h for 1 driver and 1 passenger. The driving range per charge for 2 persons at constant speed of 40 km/h requires to 80 km.

The e-scooter can be used in ASEAN cities and suburb areas, therefore the Bangkok driving cycle (BDC) [8] is

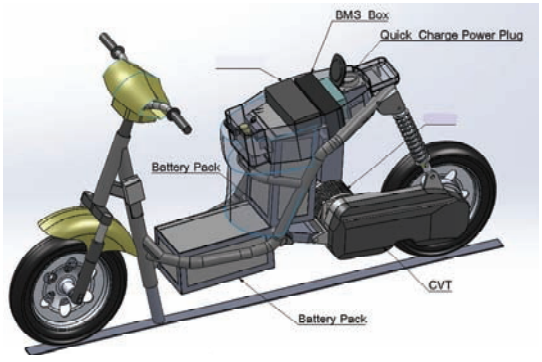

Fig. 1. Electric scooter's CAD model

† Corresponding Author: School of Electrical Engineering (SEE), Hanoi University of Science and Technology (HUST), Vietnam. (vu.trantuan@hust.edu.vn)
* Machine and Drive Design Laboratory, National Electronics and Computer Technology Center (NECTEC), Thailand. ({pakasit.somsiri, sangkla.kreuawan}@nectec.or.th)
** School of Electrical Engineering (SEE), Hanoi University of Science and Technology (HUST), Vietnam.
Received: October 3, 2017; Accepted: February 26, 2018

taken as reference. The energy consumption based on BDC and other standard driving cycle will be analyzed.

The 3D CAD model of e-scooter shows components of the electric powertrain in Fig. 1. The e-scooter is center-mounted motor with continuous variable transmission (CVT). Two battery packs with total capacity of 3 kWh are located at the footrest and inside the passenger seat.

2.2 Motor specifications and constraint requirements

The motor specifications in term of peak/continuous performances (maximum/rated torque, power and speed) are calculated from the e-scooter specification as mentioned in the previous section. Some dimension constraints are imposed e.g. external diameter and stack length.

A 48 V lithium battery pack is chosen according to the available space as well as cost constraint. Regarding to the cost of inverters, the maximum peak current is limited to 175 A. Natural cooling of the powertrain is applied due to the compact volume given. Natural air passes through the cooling fins of motor and inverter at vehicle speed.

3. Design of Electric Motors

3.1 Switched reluctance motor

In preliminary design phase, a commercial analytical software package “SPEED PC-SRD” coupled with a genetic optimization algorithm [9] gives the main dimensions of the SRM (Table 1). Motor efficiency maximization has been taken as the objective function, with respect to several constraints, for example DC voltage, maximum current fed by asymmetric half-bridge inverter, geometry constraints (diameter and stack length), torque-speed requirement. During optimization, theoretical turn-on and turn off angles are considered in the current control strategy. These angles can be used at low rotation speed, while at high speed, advanced angles are needed to overcome the back-emf and braking torque effect. These angles are optimized later on.

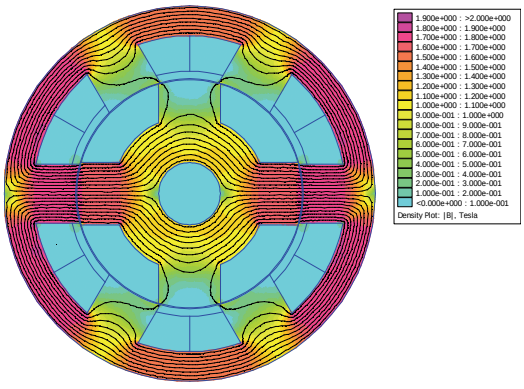

Fig. 2. SRM stator/rotor design shape and flux density at peak torque [2000rpm 14Nm]

Optimal angles result in higher torque and efficiency at the same current level.

The verification phase, conducted with an open-source finite element analysis (FEA) software “FEMM”, allows observing high flux density spots. Several magnetostatic analyses are performed with different rotor positions in order to simulate rotor rotational movement. Only one phase is excited as non-overlapped turn-on and turn-off angles are applied at this stage. The flux linkage and instantaneous torque as function of current levels and rotor positions can be verified in Fig. 2. Three-phase instantaneous torque can be computed later on by summing up all phase torques.

As mentioned above, the turn-on and turn-off angles affect motor performances. The optimized turn-on and turn-off angles are found for the whole range of motor rotation speed and torque level in order to achieve two goals, 1) high efficiency at low to medium torque and 2) maximum torque output. This yields 3 parameter look-up tables, which are used in current control strategy: turn-on angle, turn-off angle and reference current level.

3.2 Induction motor

Similar to SRM design process, the induction machine is designed base on optimal approach. Indeed, the search for the optimal solution to a problem is realized by means of sequential quadratic programming (SQP) optimization algorithm [10] coupled with an analytical model that handle constraints e.g. maximum current fed by 3-phases MOSFET inverter, battery voltage, feasible geometries, etc. The objective function aims to maximize the motor efficiency with iso-volume as SRM. The optimal motor control parameters e.g. motor voltage and slip are also taking account into in the optimal sizing step.

For an optimal sizing machine reached (Table 1 and Fig. 3), the simulations using FEA 2D transient field model with Ansys Maxwell software package are realized in order to validate this design in term of electromagnetic torque, torque oscillations, harmonic currents, and losses. Desired torque is reached by tuning slip and motor voltage.

The Indirect Field Oriented Control (IFOC) strategy [11]

Table 1. Comparison results between SRM and IM

Parameter (Unit)	SRM	IM
Total active mass (kg)	7.0	7.5
Iron mass (kg)	5.4	5.0
Copper winding (kg)	1.6	1.9
Aluminum cage (kg)	-	0.6
Outer diameter (mm)	139	139
Stack length (mm)	70	70
Air gap (mm)	0.3	0.4
Stator resistance at 20°C (mΩ)	26.6	8.8
Efficiency at constant speed at 40km/h [4600rpm 2.4Nm] (%)	85.6	90.2
Torque pulsation at [2000 rpm 13Nm] (%)	143.1	21.6
Material cost (USD)*	16.46	18.85

*: Material prices from London Metal Exchange, March 2017

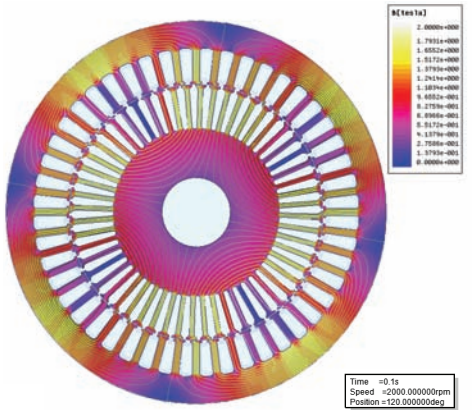

Fig. 3. IM stator/rotor design shape and flux density at peak torque [2000rpm 14Nm]

is used for induction motor drive. For each operating point in the cartography [torque and speed], a set of optimum slip and current are given in order to maximize the motor efficiency for every operating point. They are transformed into both I_d/I_q look-up tables in IFOC drive corresponding to flux and torque estimated. At high speed region, the field weakening strategy drive consists to reduce the flux to perform the torque while minimizing motor losses.

4. Design Result Comparison

SRM and IM designs are achieved as shown in Fig. 2 and Fig. 3. FEA simulations show that the optimal motors are physically correct. High magnetic saturation can be observed for both machines.

Table 1 shows optimal results for both IM and SRM motors. SRM has smaller rotor diameter, which results in less rotating mass inertia. Low rotating inertia makes SRM more suitable for high-speed operation. SRM is lighter than IM because of its shorter end winding and lack of aluminum cage. SRM's material cost is therefore lower than the one of IM.

One of SRM drawback is its high pulsation torque when controlled with traditional current profile. As result, SRM'spulsation torque is computed 143 % compared to 21.6 % for IM. In e-scooter application, this pulsation torque is less sensitive as it is attenuated by drivetrain/ transmission.

With the same outer diameter and active length, IM can operate at higher efficiency when the e-scooter cruises at constant speed of 40 km/h. That means the SRM's power density is lower than IM's one. Fig. 4 compares the efficiencies corresponding to the continuous operating points (rated required torque). The efficiencies are calculated at 80 °C winding/cage temperature. IM performs better than SRM throughout the whole speed range. One of the main loss sources is copper loss. SRM has much higher phase resistance than that of IM. IM also has fewer stray losses due to the harmonic currents

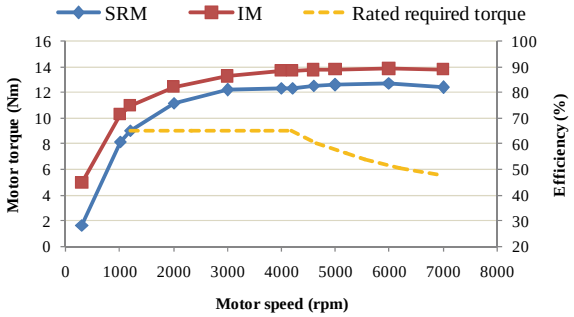

Fig. 4. Comparison of the motor efficiency corresponding to continuous operating points between SRM and IM

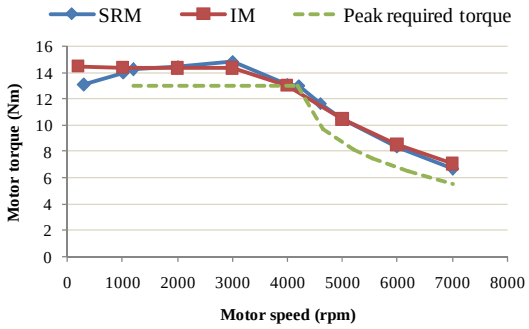

Fig. 5. Comparison of peak performances obtained by both SRM and IM designs and the specification

4.1 Peak performance results

The peak performances i.e. maximum torques corresponding to maximum motor current fed by inverter of both machines are calculated at 48 Vdc as shown in Fig. 5.

Both motors meet the peak performance requirement. In high speed field weakening regions, currents fed by the inverters can be reduced to match exactly to the specifications. This helps to improve the efficiency of the whole system. It can be seen that the IM produces more torque than SRM at stand still to very low speed, however, the maximum torque of both machines become closer at medium to high speed.

4.2 Efficiency map

The efficiency maps of both machines are calculated at iso-conditions i.e. 80°C winding/cage temperature, 175Apk maximum current fed by inverter and 48 Vdc battery voltage. The efficiency map of SRM and IM are shown in Fig. 6(a) and Fig. 6(b), respectively.

The SRM is high efficient at medium to high speed as expected. The efficiency more than 80 % is in everyday use operating zone i.e. vehicle speed of 30 – 60 km/h. The maximum efficiency is found 85.58 % at [2 Nm 7000 rpm].

IM efficiencies are higher than SRM ones. The IM efficiencies more than 80 % are located in a large area from the based speed of 2000 rpm to the top speed of 7000 rpm.

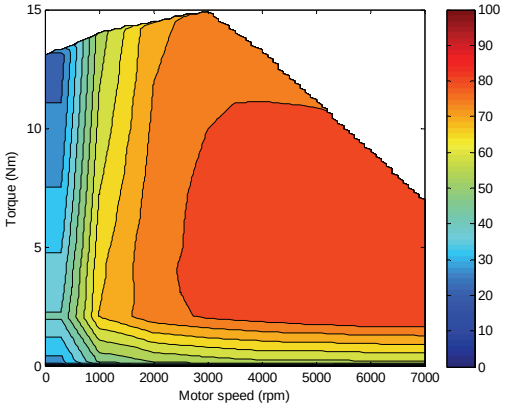

(a)

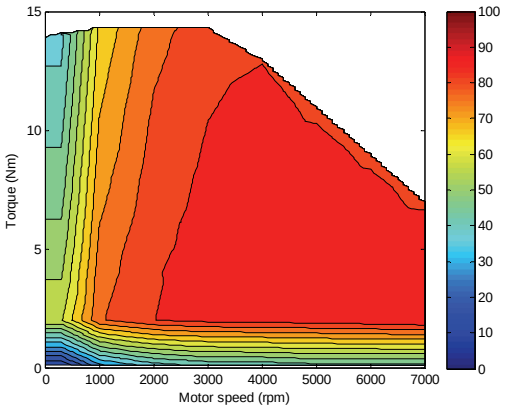

(b)

Fig. 6. Efficiency maps of (a) SRM and (b) IM

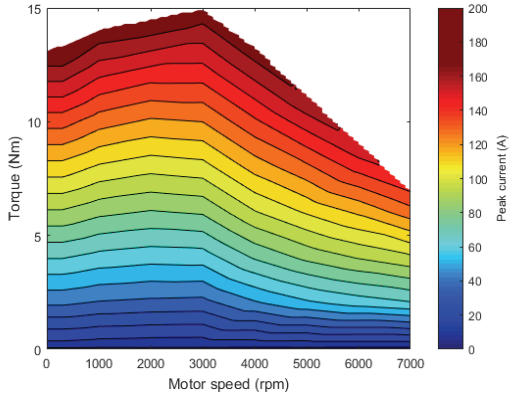

(a)

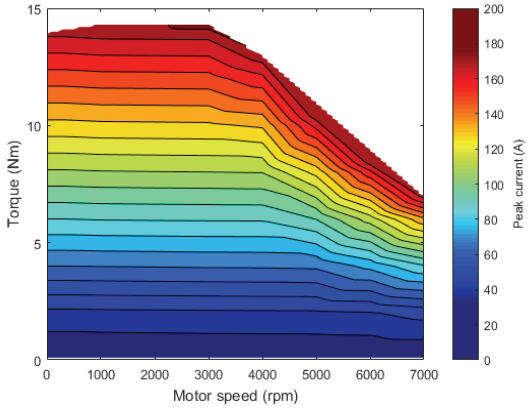

(b)

Fig. 7. Peak current map of (a) SRM and (b) IM

The maximum efficiency of IM is reached to 90.59 % at [4N.m 6000 rpm].

Both efficiency maps of SRM and IM will be used for the range calculations and comparisons in the next section.

4.3 Current map

Fig. 7 shows peak currents of each motor. It should be noted that the maximum peak current is constrained to 175 Apk for both motors.

It is noted the SRM currents contain harmonic currents due of its control strategy. Also, RMS currents depend on peak current and turn on and turn off angles. They are quite lower than IM's RMS value of sinusoidal current waveform. They are quite lower than IM's RMS value of sinusoidal current waveform.

5. Range and Performance Estimations

5.1 Bangkok driving cycle

Automotive manufacturers and automobile registration authorities use standard driving cycles for assessment of emissions, fuel consumption rates and driving range in case of electric vehicles. The standard driving cycles are for example NEDC, WLTC, ARTEMIS European, US75 or Japan 10-15 mode [12-14]. They are developed and adapted to traffic conditions in the applicable areas.

The Bangkok driving cycle (BDC) was proposed as the driving cycle representing the vehicles travelling on Bangkok's roads in the real traffic condition. The development methodology can be found in [8]. Fig. 8 shows speed-time profile of BDC. The total length is 5.71 km. It composes of multiple micro-trips. The maximum speeds of each micro-trip vary from several km/h to 62 km/h. The average speed is 17.7 km/h. The acceleration and the deceleration are 0.67 and -0.69 m/s^2, respectively. The idle time, at which the vehicle stops, is 37.7 % of the whole cycle time.

Table 2 compares different parameters for both driving cycles, BDC and ECE15 driving cycle (also known as "Elementary urban cycle" or "Urban driving cycle", UDC). It can be seen that maximum acceleration and deceleration are moderate. ECE15 cycle demands less vehicle performances, compared to BDC.

ECE15 is a European urban driving cycle, developed for emission and consumption tests. It is part of New European driving cycle (NEDC), which is composed of 4 repeated ECE15 cycles and one extra-urban driving cycle (EUDC).

Table 2. Comparison of driving cycles

Parameter (Unit)	BDC	ECE15
Length (km)	5.71	0.994
Duration (s)	1160	195
% Idle time (%)	37.7	29.2
Maximum speed (km/h)	62	50
Average speed (km/h)	17.7	18.35
Maximum acceleration (m/s^2)	2.78	1.06
Average acceleration (m/s^2)	0.67	0.64
Maximum deceleration (m/s^2)	-4.17	-0.83
Average deceleration (m/s^2)	-0.69	-0.75

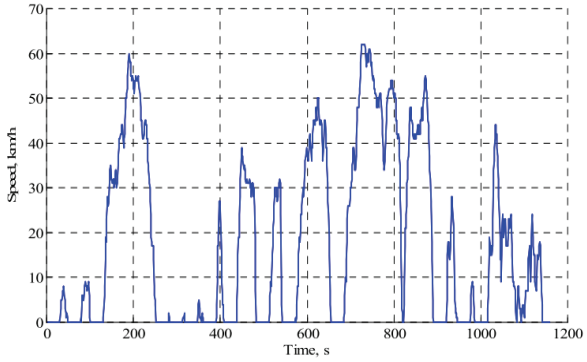

Fig. 8. Bangkok driving cycle speed-time profile [7]

NEDC's maximum speed is 120 km/h, which is not achievable by the city scooter.

It should be noted that the aforementioned driving cycles, BDC and ECE15 were originally developed for passenger cars. In the real traffic, the scooters tend to be faster than passenger cars, especially in the heavy traffic condition where the scooters can pass in between two cars. The acceleration and deceleration of scooters are also different from that of passenger cars. An improvement of BDC can be proposed for the driving cycle targeted scooters. It is an interesting topic that will improve energy consumption and range estimations of e-scooters in the future. However, it is not in the scope of this work. The original BDC and ECE15 cycles are used to simulate and compare the range of the e-scooter equipped by two different motor technologies.

5.2 Range simulation

A simulation model has been developed in Matlab/ Simulink. It is based on vehicle dynamics equations as well as each components' model e.g. battery, motor, inverter and gearbox [12]. Both forward and backward approaches [13] are used. A driver model tracks speed reference by getting vehicle speed feedback and sends torque request command to the vehicle. The torque request demand is limited by torque limit control module, which provides actual motor torque as an output.

Battery energy is then computed using backward approach from motor's actual load torque with the efficiency map in

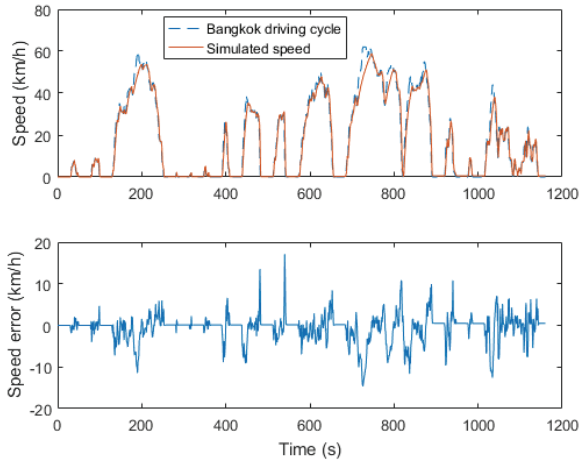

Fig. 9 Simulated speed and speed error of BDC cycle

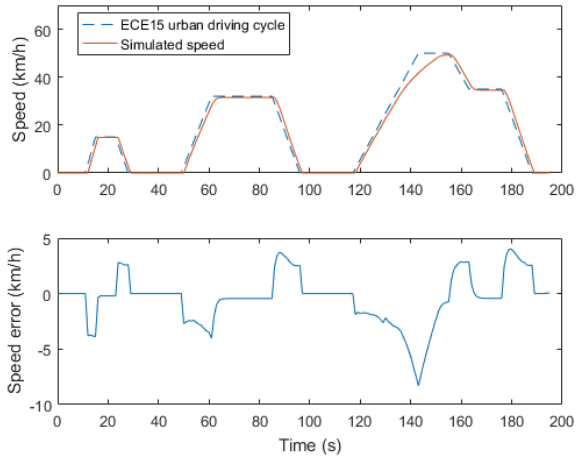

Fig. 10 Simulated speed and speed error of ECE15 cycle

Fig. 6 and inverter efficiency, which is estimated 95 %. In reality, the SRM inverter efficiency should be lower than IM one due to its lower power factor. The simulation with a driving cycle is repeated until the battery of 3000 Wh is emptied.

In the BDC and ECE15 cases, the e-scooter cannot achieve several speed and acceleration demands. The e-scooter gives inferior performances as it did not designed to meet the mentioned driving cycles. Fig. 9 and Fig. 10 show speed reference and the actual simulated e-scooter speed for BDC and ECE15 cycles. Large negative speed error means that the e-scooter has insufficient torque/power to track speed reference.

5.3 Range results

Table 3 shows range simulation results of both technologies for the e-scooter running at different scenarios i.e. BDC, ECE15, constant speed of 40 km/h, for 1 and 2 passengers. IM performs three to six km more than SRM because of its higher efficiency. For such small vehicle, one more passenger can decrease driving range

Table 3. Range (km) simulation results

Scenario	SRM	IM
Bangkok driving cycle (1 pax)	42.8	45.8
Bangkok driving cycle (2 pax)	36.1	38.8
ECE15 (1 pax)	52.0	55.1
ECE15 (2 pax)	39.6	42.5
Constant 40 km/h (1 pax)	103.1	109.1
Constant 40 km/h (2 pax)	85.1	89.9

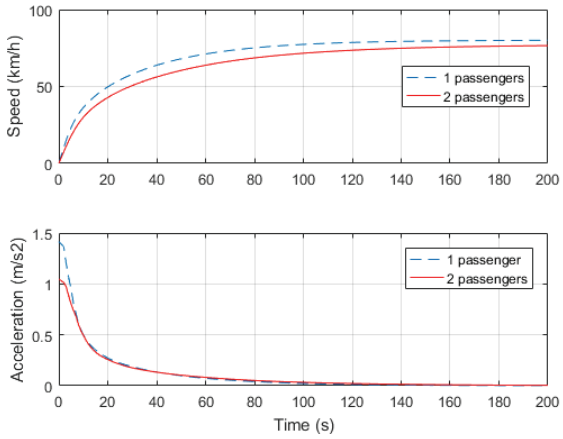

Fig. 11 Vehicle speed and acceleration to top speed

approximately from 15 % in BDC up to 23 % in ECE15 cycle. However, both motor technologies meet range requirement of 80 km at constant speed 40 km/h with 2 passengers.

The gaps of the ranges between the requirement of e-scooter specification and BDC/ECE15 scenarios are quite important because the BDC and ECE15 cycles are not adapted for city scooter.

5.4 Performance results

Both motors perform identical performances because the same maximum torque envelop is used in control algorithm.

The e-scooter's maximum speed is 80.2 km/h for one passenger and slightly decreases to 77.2 km/h with two passengers. It takes 30 to 50 s (1 and 2 passengers respectively) to accelerate from standstill to 60 km/h and then another one minute to ramp-up slowly to top speed as shown in Fig. 11.

The acceleration time from 0 – 30 km/h is 7 and 10 s for 1 and 2 passengers, respectively. Fig. 12 shows speed and acceleration of e-scooter for 0 – 30 km/h acceleration test. Other performances such as gradeabilities are also met the requirements as shown in Table 4.

5. Conclusion

The switched reluctance motor and induction motor drive systems for electric scooter are studied. They

Table 4. E-scooter performances

Parameter	1 passenger	2 passengers
Maximum speed (km/h)	80.2	77.2
Acceleration 0 – 30 km/h (s)	8	11
Maximum gradeability (%)	45	31
Gradeability at 30 km/h (%)	20.9	14.7

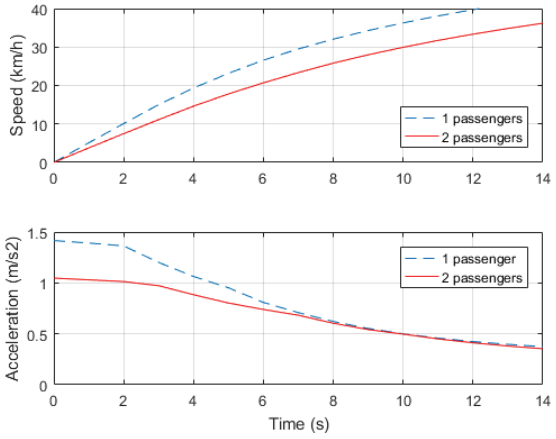

Fig. 12 Vehicle speed and acceleration from 0 to 30 km/h

provided the desired performances within the similar multi-criteria constraints. IM has better efficiency and lower pulsation torque. SRM is lighter and less expensive due to lower material cost as well as simple manufacturing process. Both types of low cost motor are considered suitable of electric city scooter application in ASEAN market. The driving ranges are analyzed based on Bangkok driving cycle, ECE15 driving cycle and at constant speed. By using a range simulation tool, the ranges can be varied from 36 to 109 km depending on cycle, technology and number of passengers. In real traffic, a driving range of 35 to 55 km can be expected. In future work, a regenerative braking strategy can be implemented. This will improve energy consumption rate of the e-scooter.

Acknowledgements

This research is supported by the Hanoi University of Science and Technology (HUST), Vietnam, T2017-TT-003 program.

References

[1] K. Kiyota and A. Chiba, "Design of Switched Reluctance Motor Competitive to 60-kW IPMSM in Third-Generation Hybrid Electric Vehicle," *IEEE Transaction Industrial Application*, vol. 48, pp. 2303-2309, Nov/Dec 2012.

[2] H. Mikami, K. Ide, Y. Shimizu, M. Senoo, and H. Seki, "Historical Evolution of Motor Technology,"

Hitachi Review, vol. 60, no. 1, 2011.
[3] D. G. Dorrell, A. M. Knight, M. Popescu, L. Evans, and D. A. Staton, "Comparison of different motor design drives for hybrid electric vehicles," *2010 IEEE Energy Conversion Congress and Exposition*, pp. 3352-3359, Atlanta 2010.
[4] G. Pellegrino, A. Vagati, B. Boazzo, and P. Guglielmi, "Comparison of Induction and PM Synchronous Motor Drives for EV Application Including Design Examples," *IEEE Transaction Industrial Application*, vol. 48, no. 6, pp. 2322-2332, Nov. 2012.
[5] B. Xia, Z. Ren, Y. Zhang, and C.-S. Koh, "An Adaptive Optimization Algorithm Based on Kriging Interpolation with Spherical Model and its Application to Optimal Design of Switched Reluctance Motor," *Journal of Electrical Engineering and Technology*, vol. 9, no. 5, pp. 1544-1550, 2014.
[6] Z. Yang, F. Shang, I. P. Brown, and M. Krishnamurthy, "Comparative Study of Interior Permanent Magnet, Induction, and Switched Reluctance Motor Drives for EV and HEV Applications," *IEEE Transactions on Transportation Electrification*, vol. 1, no. 3, pp. 245-254, Oct. 2015.
[7] M. M. Namazi, A. Rashidi, H. Koofigar, S. M. Saghaiannejad, and J-W Ahn, "Adaptive Control of Switched Reluctance Motor Drives under Variable Torque Applications," *Journal of Electrical Engineering and Technology*, vol. 12, no. 1, pp. 134-144, Jan. 2017.
[8] S. Tamsanya, S. Chungpaibulpatana, and B. Limmeechokchai, "Development of a driving cycle for the measurement of fuel consumption and exhaust emissions of automobiles in Bangkok during peak periods" *Intentional Journal Automotive Technology*, vol. 10, no. 2, pp. 251-264, Apr. 2009.
[9] S. Sivaraju, F. Ferreira, and N. Devarajan, "Genetic algorithm based design optimization of a three-phase multiflux Induction Motor," *XXth International Conference on Electrical Machines (ICEM)*, pp. 288-294, Sept. 2012.
[10] P. Venkataraman, *Applied Optimization with Matlab Programming*, A Wiley-Interscience publication, John Wiley & Sons, New York, 2002.
[11] D. D. Pinheiro, G. M. Filho, E. G. Carati, R. Cardoso, C. M. O. Stein, and J. P. da Costa, "Input command strategies and analysis for energy optimization of induction motor drives," *12th IEEE International Conference on Industry Applications (INDUSCON)*, Brazil, Nov. 2016.
[12] L. Guzzella and A. Sciarretta, *Vehicle propulsion systems: Introduction to Modeling and Optimization*, Springer Verlag, 2007.
[13] L. Horrein, A. Bouscayrol, P. Delarue, J.N. Verhille, and C. Mayet, "Forward and Backward simulations of a power propulsion system" *IFAC Proceedings Volumes*, vol. 45, no. 21, pp. 441-446, 2012.
[14] M. André, "The ARTEMIS European driving cycles for measuring car pollutant emissions," *Science of the Total Environment*, no. 334-335, pp. 73-84, 2004.

Appendix

Excitations in FEA models of SRM and IM are realized as below.

SRM windings are fed by a squarewave current:

$$I_a(\theta) = \begin{cases} 0 & ;\ 0 \le \theta < \theta_{ON} \\ I_{ref} & ;\theta_{ON} \le \theta \le \theta_{OFF} \\ 0 & ;\theta_{OFF} < \theta < \dfrac{2\pi}{n_p} \end{cases}$$

With θ mechanical rotor position, θ_{ON} turn-on angle, θ_{OFF} turn-off angle, I_{ref} current reference, n_p number of rotor pole. In SRM 6/4, this squarewave profile is repeated 4 times per one rotor revolution. For phase b and c, currents are shifted by $\pi/3$ and $2.\pi/3$, respectively.

For IM, the rotor rotation is fixed (e.g. 2000 rpm). IM windings are fed by sinusoidal voltages:

$$u_{a,b,c}(t) = U_m.sin\left(2.\pi.f_s.t - \gamma_{a,b,c}\right)$$

With f_s electric stator frequency, U_m amplitude of phase voltage, $\gamma_{a,b,c}$= 0; $2\pi/3$; 4. $\pi/3$

10 periods need to be completed in order to reach the steady state.

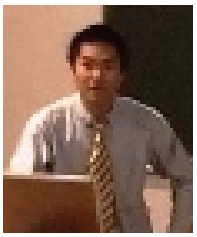

Vu Tran Tuan received Engineer Diploma (2004) from Hanoi University of Science and Technology (HUST), Vietnam, M.S. degree (2005) from Grenoble Institute of Technology and Ph.D (2009) in electrical engineering with Laboratory of Electrical Engineering and Power Electronics of Lille, France. He is currently lecturer at School of Electrical Engineering of HUST.

Sangkla Kreuawan received M.Sc. (2005) and Ph.D (2008) in electrical engineering from Laboratory of Electrical Engineering and Power Electronics of Lille, France. He is currently researcher at National Electronics and Computer Technology Center Thailand.

Pakasit Somsiri received the Bachelor degree in electronics technology from King Mongkut's Institute of Technology Ladkrabang, Thailand, in 1994, and the M.Eng. degree in electrical engineering from Thammasat University, Thailand, in 2009. He is currently a Researcher with the Machine and Drive Design Laboratory, National Electronics and Computer Technology Center, Thailand. His current research interests include switched reluctance motors and drive systems, electric drive, renewable energy and power electronics applications.

Phuong Nguyen Huy was born in Hanoi, Vietnam. He received the B.Sc (1996), M.Sc (1997) and Ph.D (2000) degree in Automation Industry from Moscow Power Engineering Institute of Russian Federation. From 2002 he joined the Department of Industrial Automation, Hanoi University of Science and Technology. His main interests include process control, control of mechatronic systems, focusing on Active Magnetic Bearing (AMB), servo motor control and Axial Self Bearing Motor (ASBM), CNC machine drive control.